Patient-specific biomechanical model of the brain: application to Parkinson's disease procedure

O. Clatz†*, H. Delingette†, E. Bardinet†‡, D.Dormont‡ and N. Ayache†

†:Epidaure Research Project, INRIA Sophia Antipolis
2004 route des Lucioles, 06902 Sophia Antipolis, France
‡Neuroradiology Dept and LENA UPR 640-CNRS La Pitié-Salpêtrière hospital
91, 105 boulevard de l'Hôpital 75013 Paris, France
*Corresponding author: Olivier.Clatz@inria.fr

Abstract. Stereotactic neurosurgery for Parkinson's disease consists of stimulating deep nuclei of the brain. Although target coordinates are calculated with high precision on the pre-operative images, cerebrospinal fluid (CSF) leakage during the procedure can lead to a brain deformation and cause potential error with respect to the surgical planning. In this paper, we propose a patient-specific biomechanical model of the brain able to recover the global deformation of the brain during this type of neurosurgical procedure. Such a model could be used to update the pre-operative planning and balance the mechanical effects of the intra-operative brain shift.

1 Introduction

It is usually the case in neurosurgery that pre-operative planning is based on the assumption that anatomical structures do not move between the image acquisition time and the operation time. In reality, the position of brain tissues changes during the operation and significantly decreases the accuracy of the planning made on the pre-operative image. Two approaches have been proposed to solve this problem. One uses intra-operative images (ultra-sound devices [7], stereo-vision systems [8], open-configuration magnetic resonance scanners [3]) to register the pre-operative images with the intra-operative ones. The second one attempts to predict the brain deformation. This approach can be either based on statistical models [2] or on biomechanical models [5].

The biomechanical approach we propose here is based on a finite element model (FEM) of the brain. It takes into account the patient specificity and anatomical cerebral structures to predict the brain deformation.

2 Stereotactic neurosurgery for Parkinson's disease

2.1 Overview of the surgical procedure

The Parkinson's disease procedure consists of the deep implantation of electrodes to stimulate the subthalamic nuclei in the brain. It recently renewed the interest for functional stereotactic surgery.

This method uses a metallic non-magnetic stereotactic frame visible on the different imaging modalities (T1, T2, scanner) as a geometrical referential fixed on the patient's head. The frame serves as a guide for the electrodes paths during the procedure. After locating the target nuclei on pre-operative images, the path of electrodes is planned through the parenchyma, avoiding crossing critical structures like sulci, blood vessels or ventricles. We notice that no consensus quo has been reached yet in the definition of these critical structures. The surgical procedure starts the day after the planning. The surgeon first makes two holes in the skull for accessing the two hemispheres but perform the electrodes implantation one after the other. Because all images in this study come from a single surgeon, the hemispheres are treated in the same order for every patient. After the dura mater opening, the surrounding zone around the target nuclei is explored in a $\pm 5mm$ zone around the pre-operative located position by five different electrodes testing each position to determine the best stimulating location. However, depending on the intervention duration (6 to 10 hours) and on the dura-mater opening size, the CSF leakage induces a brain deformation which might compromise the localization of the targeted nucleus.

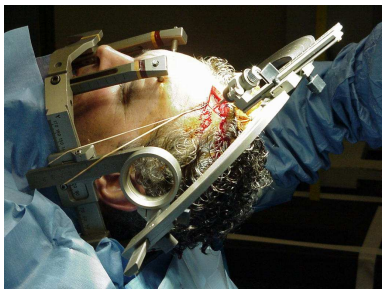

Fig. 1. Stereotactic operation at La Pitié Salpêtrière hospital (courtesy of Medtronic Inc).

2.2 The data

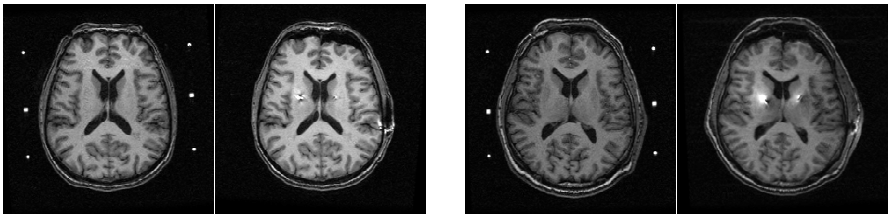

pre-op post-op pre-op post-op

Fig. 2. Two cases extracted from the seven pre and post operative T1 weighted MRI used for this study.

This study is based on the analysis of 7 cases of Parkinson's disease treated at La Pitié Salpétrière hospital in Paris. The images considered for this study are T1 weighted MRIs (IR-FSPGR). The 7 cases are staggered over two years between 1999 and 2001. All patients have been operated following the same

protocol: the pre-operative images and planning are performed the day before the procedure while the procedure starts early in the morning, following the previously described protocol, and in the same position. The post-operative MRI images are acquired in the morning of the day after the procedure. The patient is kept lying down until the post-operative image acquisition. (figure 2).

3 Methods

The model we propose is based on a retrospective study of the deformation measured on the 7 patients, rigidly registered on an atlas in a pre-treatment stage (see [6] for the rigid registration algorithm. Figure 3 presents an overview of the proposed method. The model creation can be decomposed in different steps :

- brain segmentation
- patient pre to post-operative deformation generation
- deformation analysis and characteristic features extraction
- patient specific biomechanical model building
- model parameters optimisation

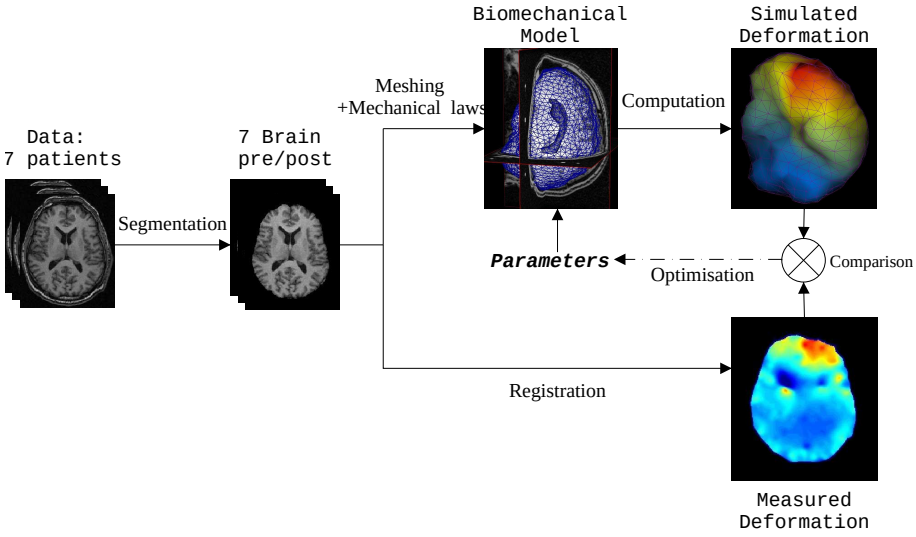

Fig. 3. Overview of the proposed method

3.1 Displacement field extraction from the non-rigid registration

Brain parenchyma segmentation We developed a simple automatic method based on the registration of a digital atlas [1] on the pre/post operative MRI. The overall method is presented in figure 4.

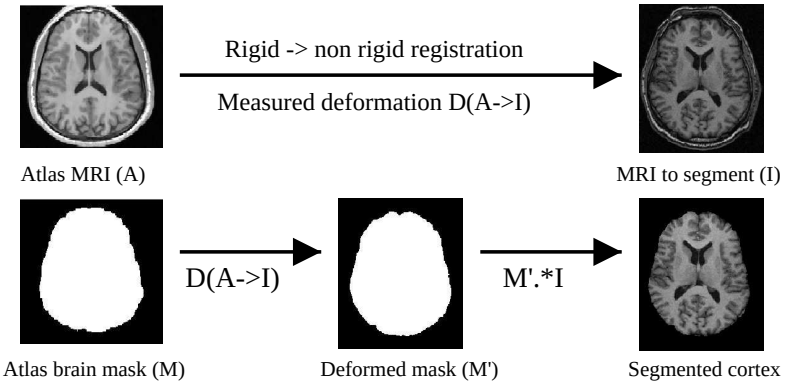

Fig. 4. Brain segmentation method

To optimize the precision of the registration procedure, we split it into different stages, with increasing complexity, initializing each displacement field by the previously computed one :

$$\text{similarity [6]} \Longrightarrow \text{affine [6]} \Longrightarrow \text{free-form [1]}$$

Finally, we used the final free-form displacement field obtained from the registration software to deform the brain mask.

Building an average displacement field In order to analyze the deformations that occur in the brain, we compute the non rigid displacement field between each pre and post-operative MRI from the 7 cases of Parkinsonians, already rigidly registered in the atlas geometry. The average displacement field is then built by averaging these 7 displacement fields (figure 5).

3.2 Characteristic feature extraction

Displacement analysis One can, from these first displacement fields generated, put forward different phenomena:

[1] http://splweb.bwh.harvard.edu:8000/pages/papers/atlas/

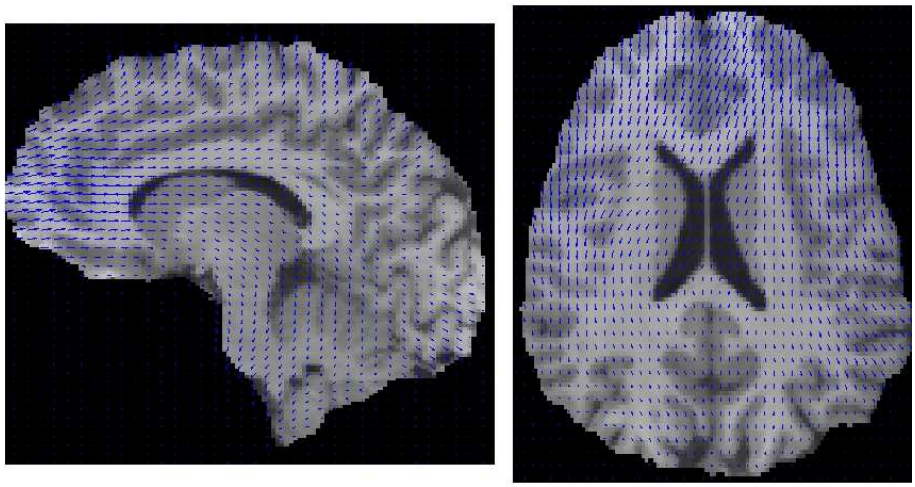

Fig. 5. Average displacement field computed over the 7 cases, affine registered on the atlas brain.

- assuming an horizontal position of the patient in the MRI scanner, we computed the average displacement direction. This one is mostly aligned with the gravity (average direction difference = 17^o).
- we observed for almost every cases an important asymmetry in the displacement field of the two hemispheres (also distinguishable on the pre and post-operative MRIs, see figure 2).

The metallic nature of the electrodes introduces very important artifacts on the computed displacement fields, so that we cannot make any deformation analysis on this area.

Deformation analysis Let $\boldsymbol{\Phi}$ denote the relationship which associates the new position vector of a material point $\mathbf{X}$ to its rest position after transformation in a fixed reference. $\mathbf{U}(\mathbf{X})$ is the displacement function.

$$\boldsymbol{\Phi}(\mathbf{X}) = \mathbf{X} + \mathbf{U}(\mathbf{X}).$$

We can then compute the image (figure 6) which represents the local volume variation (defined by the ratio of the local volume variation by the initial volume) :

$$\frac{d\Omega - d\Omega_0}{d\Omega_0} = det(\nabla \boldsymbol{\Phi}(\mathbf{X})) - \mathbf{1} = det(\mathbf{Id} + \nabla \mathbf{U}(\mathbf{X})) - \mathbf{1}$$

This new image (6) revealed an incompressible behavior for the brain parenchyma, with a compression rate comprised between +5% and -5%, except in the electrode area where artifacts induced large unrealistic compression rate values (over 15%).

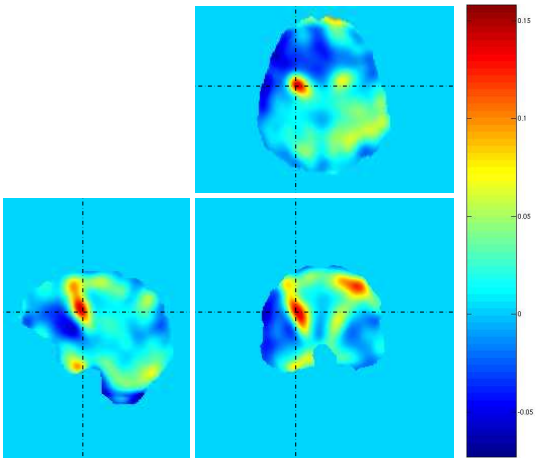

Fig. 6. Local deformation rate : $\frac{d\Omega - d\Omega_0}{d\Omega_0}$.

4 The biomechanical model

To build a physically-based deformable model, one must follow different steps. After the generation of a tetrahedral mesh (4.1), we have to choose a biomechanical constitutive behavior law for the brain material, based on continuum mechanics laws (4.2). The next step is boundary conditions determination, depending on the observed behavior (4.3). Last step is the computation of the solution (4.4).

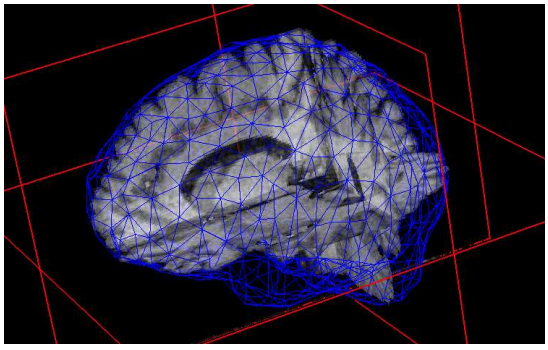

Fig. 7. Final tetrahedral mesh of the brain

4.1 Mesh generation

We use the masks of the brain presented in section 3.1 to generate the volumetric mesh (figure 7) with the package GHS3D developped at INRIA Rocquencourt[2]. This software minimizes the shape variability between all tetrahedra in the final mesh. We limited the number of tetrahedra in the model to 8000, in order to keep the computation time under two minutes. The proposed method allows us to automatically create a patient-specific mesh of the cortex (figure 7).

4.2 Material parameters

We propose a model for brain tissue material which takes into account the observation made on the deformation :

1. We assume a brain tissue material almost incompressible, which is consistent with the known mechanical properties of the brain parenchyma [4] and with the deformation analysis made in section 3.1. We have thus fixed its Poisson ratio to 0.45.
2. With no a-priori information about the brain tissue stiffness, we used the Young Modulus measured in Karol Miller experiments (See [4] for more details) $E = 2000Pa$. We can then compute the Lamé constants :

$$\mu = 689 \quad \lambda = 6200$$

3. In a first stage, we assumed an isotropic material, with linear elasticity behavior law. We wish to insist on the fact that this kind of behavior law does not aim to model a dynamic behavior (like viscoelastic) but only the static effects of an external loading.

4.3 Boundary conditions

With respect to the displacement field obtained in section 3.1 we propose a new model including the brain anatomy and the mechanics of static fluids.

1. We consider that a Cerebro Spinal Fluid leak leads to an equivalent liquid level in the skull. The brain part under this liquid level is then subject to the fluid force applied on the brain surface and the gravity :
   - The local volumetric force induced by gravity is:

$$\mathbf{F}_{Gravity} = -\int_{Brain\ Volume} \rho\, \mathbf{g}\, dV$$

   ρ is the mass density of the brain ($\simeq 1Kg.dm^{-3}$)
   $\mathbf{g}$ is the gravity vector ($|\mathbf{g}| = 9.81N.Kg^{-1}$)

[2] http://www-rocq1.inria.fr/gamma/index.html

– Considering no friction between the brain and the skull, the force of the fluid applied o the brain is :

$$\mathbf{F}_{Fluid} = \iint_{Brain\ Surface} P_{fb}\, dS = \iiint_{Brain\ Volume} grad(P_{fb})\, dV$$

P_{fb} is the pressure of fluid on the brain
The explicit pressure law in a fluid is given by:

$$P_{fb} = \rho\, g\, h + P_0$$

h is the distance to the liquid level
P_0 is the air pressure

$$\text{Then: } \mathbf{F}_{Fluid} = \iiint_{Brain\ Volume} \rho\, g\, dV$$

Therefore, if no friction exists between the brain and the skull, we can consider that the resultant force applied to the part of the brain under the liquid level is null.

2. The part of the brain which is over the liquid level is subject to gravity only ($\int P_0$ is balanced over the total surface of the emerged part). On each tetrahedron's vertex, we have then applied the force :

$$\mathbf{F} = \Sigma_{Adjacent\ Tetrahedron}(-\iiint_{Tetrahedron\ Volume} \frac{\rho\, g\, dV}{4})$$

3. To take into account the asymmetry in the computed displacement field, we propose to separate the hydraulic behavior of each hemisphere. This hypothesis is based on the anatomy (the falx cerebri). It is also based on the fact that during a this type of neuro-surgical procedure, the two hemispheres are treated one after the other. We have then a different CSF liquid level for each hemisphere leading to two different volumetric forces applied to each hemisphere.
4. To balance the force moment due to the difference of forces between both sides, we implicitly modeled the falx cerebri, allowing vertices belonging to tetrahedron intersecting the mid-sagittal plane to slide along this plane.
5. Finally, we fixed vertices at the basis of occipital lobe (on 10 % of the total height) since displacement analysis showed no displacement for this part of the brain.

4.4 Numerical solving of the mechanical problem

Once boundary conditions have been applied, we have to solve the linear system :

$$[\mathbf{K}]\ \mathbf{U} = \mathbf{F}$$

$[\mathbf{K}]$ Stiffness matrix
$\mathbf{U}$ Displacement vector
$\mathbf{F}$ External force vector

We do not explicitly compute the stiffness matrix inverse $[\mathbf{K}]^{-1}$. Due to the sparseness of $[\mathbf{K}]$, we precondition the $[\mathbf{K}]$ matrix with incomplete Cholesky method using tools of the Matrix Template Library[3]. The final solution is obtained with the conjugate gradient method of the Iterative Template Library[4].

5 Results

Matching criterion To estimate the quality of the prediction, we need to have an error criterion sensitive not only to voxel-value error, but also to displacement error over the brain. We propose to compute the sum of squared displacements over the brain obtained by registering the predicted MRI with the post-operative MRI:

$$Error = \iiint_{Brain\ Volume} \left| \overrightarrow{\hat{u}} \right|^2 .dV$$

where $\overrightarrow{\hat{u}}$ is the measured displacement.
This criterion, more than a precise estimate of the real displacement error, is used as an energy function we minimize to adjust our model's parameters which best correspond to the target post-operative image.

Model performance evaluation We performed our model tests in two stages: first, we optimized an average CSF liquid level in the skull with respect to our matching criterion (the optimum value is 18.5%), then we computed the two different CSF liquid levels, initializing the two levels with the optimal average one.

Figure 8 presents the absolute difference of pre and post-operative MRI compared to the absolute difference of predicted and post-operative MRI. The predicted MRI have been computed with the two CSF liquid levels that minimize the global error with the post operative MRI. We can verify that our model is able to balance the brain shift phenomenon as well as the asymmetry. Nevertheless, the model does not seem to reduce the difference residue on the sulcus area. This problem is, in our opinion, due to the homogeneous material model proposed for the full brain and maybe also to displacement boundary conditions imposed at the base of the occipital lobe.

The observation of the image difference allows us to evaluate the quality of the biomechanical prediction:

- The model relates well to asymmetrical deformation.
- The gravity-induced deformation is quantitatively well modeled by the physically-based biomechanical model we propose.

[3] http://www.osl.iu.edu/research/mtl/
[4] http://www.osl.iu.edu/research/itl

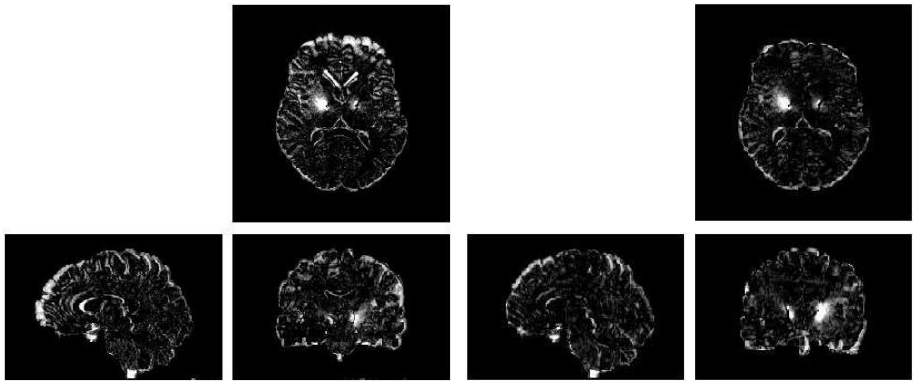

Difference pre / post-operative MRI Difference predicted / post-operative MRI.

Fig. 8. Comparison of the difference images with and without prediction (patient with the largest brain-shift).

- As previously seen, the measured displacement is very disturbed in the electrode area. We thus have no way to estimate the accuracy of the displacement in this area.
- We observed a general error increase from the center of the brain to its surface, which might originate from the incompressibility constraint.
- Finally, we can see on the sagittal view of the right block of figure 8 that the predicted displacement in the pre-motor area of the frontal lobe is significantly higher than the real one. We therefore propose to prevent the brain to move too far in this direction by modeling the **contact with the skull** in our model.

6 Discussion

This paper demonstrates the ability of a biomechanical model to predict gravity-induced deformations of the brain. The model shows good results for the global displacement and the asymmetrical effects for both brain surface and ventricles. However it still has some weaknesses, especially for the displacement of the frontal lobe. Actually, this displacement observation reveals that the brain collides with the skull in the pre-motor area of the frontal lobe. We thus need to improve our model with a brain/skull contact model.

Discussions with surgeons also revealed the leading role of physiological parameters on the mechanical behavior of the brain. Effects of the mannitol (a drug administered to the patient during the surgery), could explain for instance some of the errors measured on the brain surface. Thus drug effects might balance the mechanical incompressibility constraint. These kind of physiological reaction need to be taken into account in future models.

Using a physics-based model seems to be well suited to explaining the real deformations measured on pre-operative and post-operative MRIs. Although the

model cannot predict the entire deformation yet, we believe these are encouraging preliminary results. Further work will include other anatomical structures to simulate more complicated procedures. Combining anatomical and physiological constraints will help understanding and simulating the brain deformation in the future.

References

1. P. Cachier, E. Bardinet, D. Dormont, X. Pennec, and N. Ayache. Iconic Feature Based Nonrigid Registration: The PASHA Algorithm. *CVIU — Special Issue on Nonrigid Registration*, 2003. In Press.
2. C. Davatzikos, D. Shen, A. Mohamed, and S. Kyriacou. A framework for predictive modeling of anatomical deformations. *IEEE Trans. on Med. Imaging*, 20(8):836–843, 2001.
3. Matthieu Ferrant, Arya Nabavi, Benoît Macq, Black P.M., Ferenc A., Jolesz, Ron Kikinis, and Simon K. Warfield. Serial registration of intraoperative mr images of the brain. *Medical Image Analysis*, 6(4):337–360, 2002.
4. Miller K. *Biomechanics of Brain for Computer Integrated Surgery.* Warsaw University of Technology Publishing House, 2002.
5. M. I. Miga, K. D. Paulsen, J. M. Lemry, F. E. Kennedy, S. D. Eisner, A. Hartov, and D. W. Roberts. Model-updated image guidance: Initial clinical experience with gravity-induced brain deformation. *IEEE Trans. on Med. Imaging*, 18(10):866–874, 1999.
6. A. Roche, A. Guimond, N. Ayache, and J. Meunier. Multimodal Elastic Matching of Brain Images. In *Computer Vision - ECCV 2000*, volume 1843 of *LNCS*, pages 511–527, Dublin, Irlande, June 2000. Springer Verlag.
7. A. Roche, X. Pennec, G. Malandain, and N. Ayache. Rigid registration of 3D ultrasound with MR images: a new approach combining intensity and gradient information. *IEEE Transactions on Medical Imaging*, 20(10):1038–1049, October 2001.
8. Oskar Skrinjar, Arya Nabavi, and James Duncan. Model-driven brain shift compensation. *Medical Image Analysis*, 6(4):361–374, 2002.